amplifier. In: The international topic meeting on microwave photonics, 2011, 77–80.
10. K.H. Lee, J.Y. Kim, and W.Y. Choi, Injection-locked hybrid optoelectronic oscillators for single-mode oscillation, IEEE Photon Technol Lett, 20 (2008), 1645–1647.
11. O. Okusaga, W.M. Zhou, and E. Levy, Experimental and simulation study of dual injection-locked OEOs, In: Frequency Control Symposium, 2009, 875–879.
12. H.K. Sung, E.K. Lau, X.X. Zhao, D. Parekh, and J. Connie, Optically injection-locked optoelectronic oscillators with low RF threshold gain, In: Conference on Lasers and Electro-Optics, 2007, 1–2.



# DUAL-FEED SMALL-SIZE LTE/WWAN STRIP MONOPOLE ANTENNA FOR TABLET COMPUTER APPLICATIONS

**Po-Wei Lin and Kin-Lu Wong**
Department of Electrical Engineering, National Sun Yat-sen University, Kaohsiung 80424, Taiwan; Corresponding author: wongkl@ema.ee.nsysu.edu.tw

*Received 25 February 2013*

**ABSTRACT:** *A small-size strip monopole antenna with dual feeds disposed at one corner of the supporting metal plate of the display of the tablet computer for LTE/WWAN operation is presented. The strip monopole is configured into a simple inverted-L shape of 29 mm (less than 0.08 wavelength at 750 MHz) and has a low profile of 10 mm above the two side edges of the corner. A first end of the strip monopole can be connected to a first ON/OFF switch (switch-1) for lower-band operation, while a second end of the strip monopole can be connected to a second ON/OFF switch (switch-2) for higher-band operation. When switch-1 is ON with switch-2 OFF, the antenna is fed at port-1. In this case, with the aid of a wideband matching circuit, the antenna can provide a wide lower band to cover the LTE band13 and GSM850/900 operation (746–960 MHz). When switch-1 is OFF with switch-2 ON, the antenna is fed at port-2 and can provide a wide higher band to cover the GSM1800/1900/UMTS/LTE2300/2500 operation (1710–2690 MHz). Good radiation characteristics for frequencies over the antenna's operating bands are also obtained. Operating principle of the antenna is described in the article. Experimental results and parametric studies of the antenna are presented.* © 2013 Wiley Periodicals, Inc. Microwave Opt Technol Lett 55:2571–2576, 2013; View this article online at wileyonlinelibrary.com. DOI 10.1002/mop.27890

**Key words:** *mobile antennas; LTE/WWAN antennas; tablet computer antennas; small antennas*

## 1. INTRODUCTION

For the traditional internal handheld device antennas, in order to generate resonant modes in the desired operating bands, the radiating metal strips thereof are generally required to have a length of about 0.25 wavelength of a frequency in the operating band [1]. This greatly limits the size reduction of the internal antennas embedded inside the handheld devices. Recently, it is shown that by placing a small patch near the system ground plane of a mobile handset [2], an asymmetric dipole structure formed by the small patch and the system ground plane can be successfully excited with the aid of wideband matching circuits [2,3]. Wide operating bands covering either the 824–960 or 1710–2690 MHz bands can be obtained. For covering both the 824–960 and 1710–2690 MHz bands, two small patches of size $6 \times 6$ mm$^2$ can be disposed at two corners of an edge of the system ground plane [2]. In this case, even with the inclusion of the clearance region between the two small patches, such an internal LTE/WWAN antenna is attractive for practical applications.

In this article, we present a small-size strip monopole antenna with dual feeds disposed at one corner of the supporting metal plate of the display of the tablet computer for LTE/WWAN operation. The strip monopole is configured into a simple inverted-L shape of 29 mm (less than 0.08 wavelength at 750 MHz) and has a low profile of 10 mm above the two side edges of the corner. With the aid of a wideband matching circuit, although the strip monopole has a very small size, the proposed antenna can generate two wide operating bands to cover the LTE band13/GSM850/900 (746–960 MHz) and GSM1800/1900/UMTS/LTE2300/2500 (1710–2690 MHz) operations.

The antenna's lower and higher bands are generated by feeding the antenna at its first and second ends, respectively, which are located at two opposite edges of the strip monopole. To control the excitation of the lower and higher bands, each end can be connected to an ON/OFF switch (e.g., a switching diode [4–6]), which for simplicity in this study is replaced by a simple metal strip for the ON state (the forward-biased state) and an open gap for the OFF state (the reverse-biased state). As shown in [6], the results for the two cases of the antenna with PIN diodes and conducting tapes for the desired ON/OFF states show very small variations.

In the proposed design, when one switch is ON and another switch is OFF, either the first end is excited for the lower-band operation or the second end is excited for the higher-band operation. For the lower-band excitation, the wideband operation is achieved with the aid of a wideband matching circuit. Conversely, for the higher-band excitation, owing to the resonant length of the strip monopole selected to be close to 0.25 wavelength of a frequency in the desired 1710–2690 MHz band, no matching circuits are needed in aiding the resonant mode excitation for the antenna's higher band, and wideband operation of the higher band is also obtained in this study. Detailed operating principle of the proposed antenna is described in this article, and a parametric study for major parameters of the antenna is presented. Results of the fabricated antenna are also shown.

## 2. PROPOSED ANTENNA AND PARAMETIC STUDY

The geometry of the proposed dual-feed LTE/WWAN antenna is shown in Figure 1. The antenna mainly comprises a simple inverted-L strip monopole and is disposed at one corner of the supporting metal plate of the display of the tablet computer. The dimensions of the supporting metal plate are selected to be $150 \times 200$ mm$^2$, which is a reasonable size for a tablet computer with a 10-inch display panel. As shown in the figure, the first end (point A) of the inverted-L strip can be connected to a first ON/OFF switch (switch-1) through a narrow strip AA′ (width 0.5 mm, length 1.5 mm), while the second end (point B) can be connected to a second ON/OFF switch (switch-2) through a narrow strip BB′ (width 0.5 mm, length 1.5 mm). Switch-1 further connects to a wideband matching circuit [2] and controls port-1 excitation to generate a lower band for the antenna. Conversely, switch-2 controls port-2 excitation to generate a higher band for the antenna, and no matching circuits are needed for port-2 excitation.

The inverted-L strip has a width of 6.5 mm and a length of 29 mm, which is only about 0.073 wavelength at 750 MHz. When switch-1 is ON (simulated as a 2-mm long metal strip) and switch-2 is OFF (simulated as a 2-mm long gap), the antenna is fed at port-1 and has an open end at point B′. In this case, the resonant length of the antenna is much less than 0.25

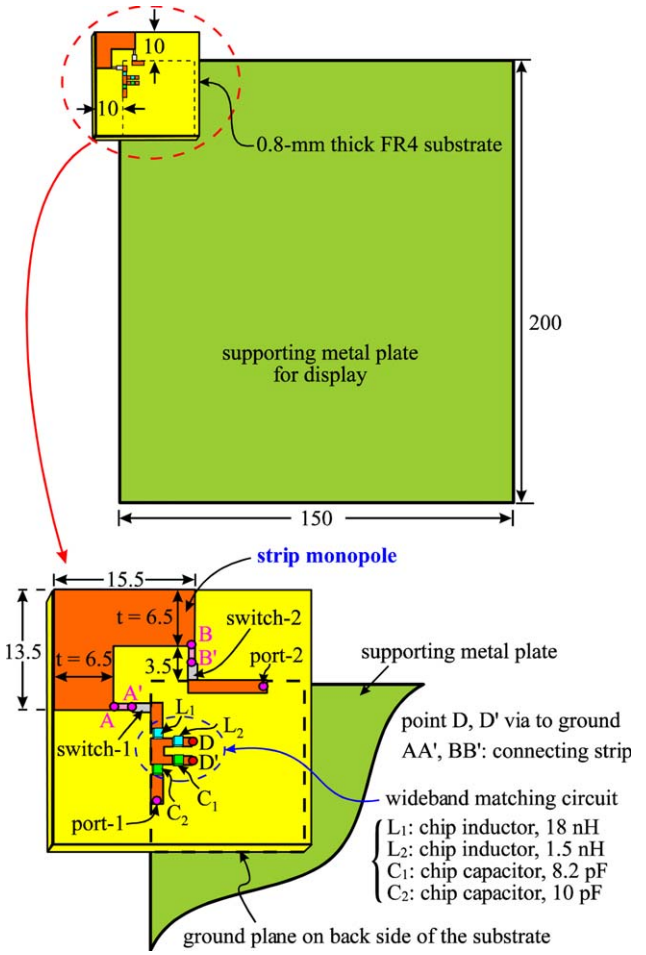


**Figure 1** Geometry of the dual-feed LTE/WWAN strip monopole antenna for tablet computer applications. [Color figure can be viewed in the online issue, which is available at wileyonlinelibrary.com]

wavelength of the frequencies in the desired lower band at about 800 MHz. With the aid of the wideband matching circuit with a series chip inductor (18 nH), a shunt chip inductor (1.5 nH), a shunt chip capacitor (8.2 pF), and a series chip capacitor (10 pF), a wide lower band covering LTE band13/GSM850/900 operations is obtained. The simulated return-loss results obtained using the full-wave electromagnetic field simulator HFSS version 14 [7] for antenna's port-1 and port-2 excitation are shown in Figure 2. Based on 6-dB return loss which is widely used as one of the design specifications of the internal handheld device antennas [8,9], the lower band can cover the desired lower-band

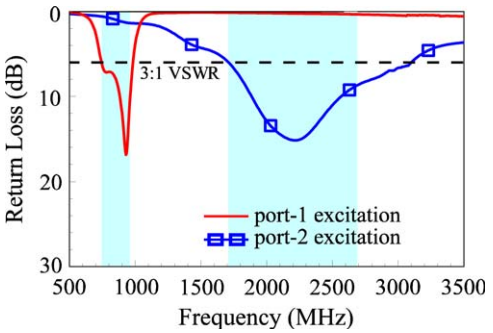


**Figure 2** Simulated return loss for the antenna. [Color figure can be viewed in the online issue, which is available at wileyonlinelibrary.com]

operation of 746–960 MHz (the shaded frequency range at lower frequencies in the figure). A typical case for the excited surface current distributions at 925 MHz on the antenna and the supporting metal plate is also shown in Figure 3.

For port-2 excitation (switch-2 ON simulated as a 2-mm long metal strip and switch-1 OFF simulated as a 2-mm long gap), a very wide higher band of about 1710–3100 MHz is obtained. As discussed earlier, no matching circuits are required for port-2 excitation. The obtained higher band covers the GSM1800/1900/UMTS/LTE2300/2500 operations (the shaded frequency range at higher frequencies in the figure). A typical case for excited surface current distributions at 1920 MHz for port-2 excitation is also shown in Figure 3. Results indicate that the proposed design can effectively control the port-1 and port-2 excitation of the antenna.

Figure 4 shows the simulated antenna efficiency which is the total efficiency including the mismatching losses. For frequencies in the lower and higher bands, the antenna efficiency is about 56–84% and 72–95%, respectively. The obtained antenna efficiency is good for practical applications.

Effects of the wideband matching circuit on the antenna's return loss for port-1 excitation (switch-1 ON, switch-2 OFF)

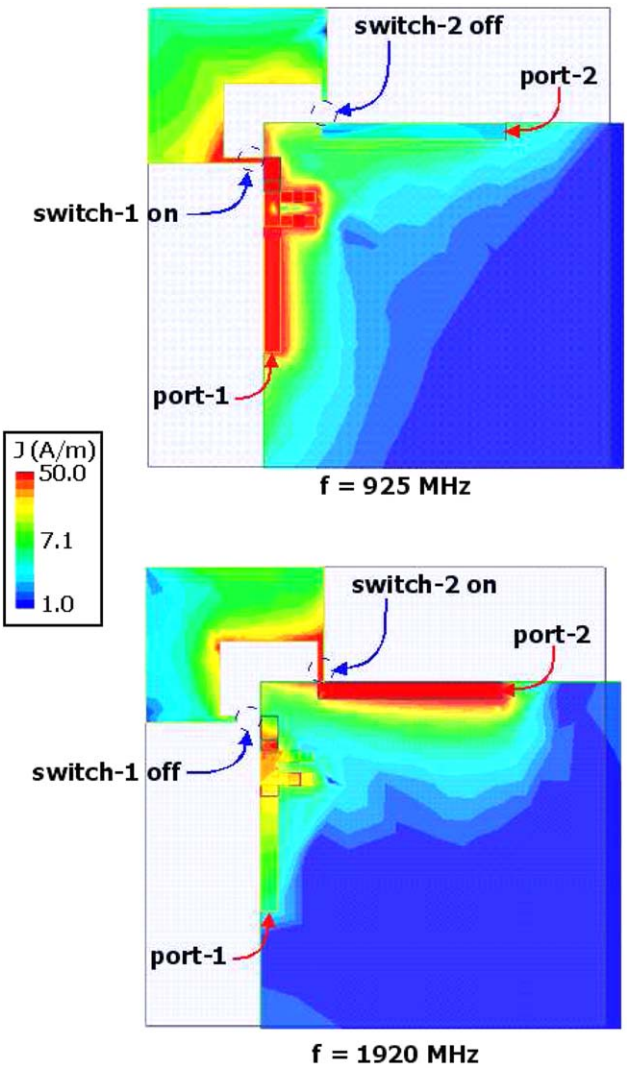


**Figure 3** Simulated surface current distributions at 925 and 1920 MHz for the antenna. [Color figure can be viewed in the online issue, which is available at wileyonlinelibrary.com]

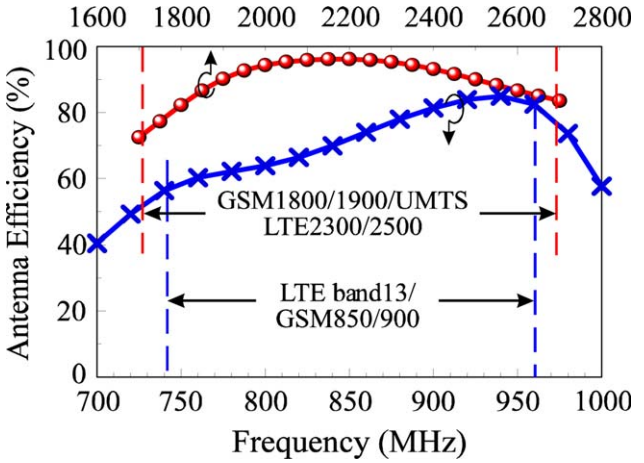


**Figure 4** Simulated antenna efficiency (mismatching losses included). [Color figure can be viewed in the online issue, which is available at wileyonlinelibrary.com]

are shown in Figure 5. First note that when all the elements of the matching circuit are not present (i.e., the case without $L_1$, $L_2$, $C_1$, $C_2$), the return loss for port-1 excitation is generally about the same as that for port-2 excitation. In this case, the desired lower band cannot be obtained. With the series chip inductor of $L_1$ only, the excited resonant mode can be shifted to lower frequencies close to 900 MHz, yet with narrow bandwidth. By further adding the shunt chip inductor $L_2$ and chip capacitor $C_2$, the resonant mode can have a dual-resonance behavior to greatly widen the bandwidth of the antenna's lower band. The series chip capacitor $C_1$ fine adjusts the impedance matching for frequencies in the desired lower band.

Effects of the strip width on the antenna's operating bands are also studied. Figure 6 shows the simulated return loss for the strip width $t$ varied from 4.5 to 7.5 mm. Small effects of the strip width on the lower band are seen. Conversely, large effects on the higher band are observed. The higher band is shifted to higher frequencies with a larger bandwidth when the strip width is increased. The frequency shifting is owing to the decreased effective resonant length for the strip monopole with a wider width. Also, a wider strip width can make the excited surface current distribution become smoother on the strip monopole, thereby resulting in a wider bandwidth. In the proposed design,

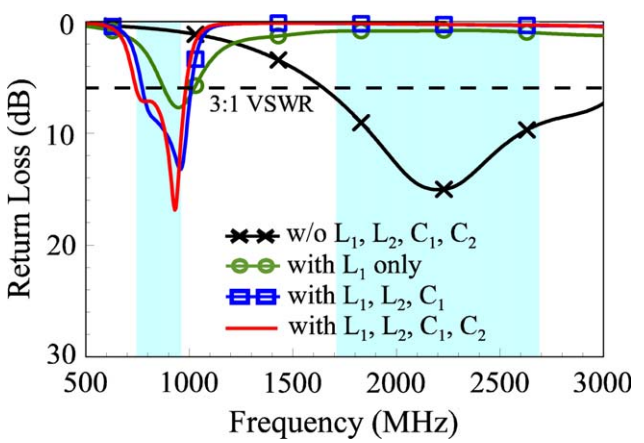


**Figure 5** Simulated return loss showing the effects of the wideband matching circuit for the antenna with port-1 excitation. [Color figure can be viewed in the online issue, which is available at wileyonlinelibrary.com]

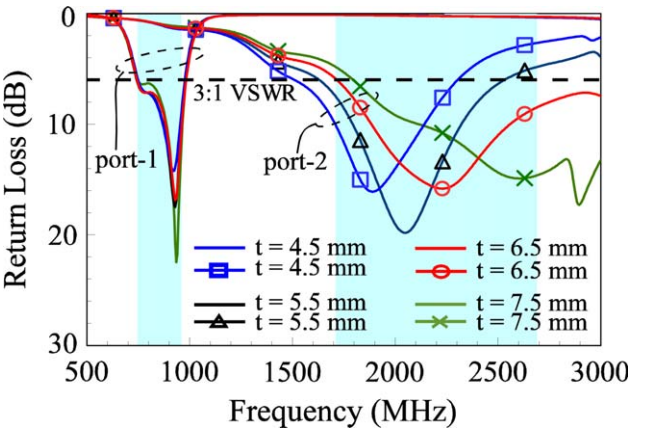


**Figure 6** Simulated return loss as a function of the strip width for the antenna. [Color figure can be viewed in the online issue, which is available at wileyonlinelibrary.com]

the strip width is chosen to be 6.5 mm such that the desired lower band (746–960 MHz) and higher band (1710–2690 MHz) are covered.

Figure 7 shows the simulated return loss for the supporting metal plate size varied from 150 × 200 mm$^2$ to 150 × 150 mm$^2$. In this study, the long edge of the supporting metal plate is varied from 200 to 150 mm, while the short edge is fixed to 150 mm. Other dimensions of the proposed design are the same as shown in Figure 1. It is seen that there are small variations in the impedance matching of the antenna, and the obtained bandwidths can still cover the desired lower and higher bands. The results suggest that the proposed design is not sensitive to the supporting metal plate size.

## 3. MEASURED RESULTS AND DISCUSSION

The antenna was fabricated and tested. Figure 8 shows the photos of the fabricated antenna with a metal plate size of 150 × 200 mm$^2$. The metal plate is cut from a 0.2-mm thick copper plate. The antenna dimensions are given in Figure 1. For port-1 excitation [Fig. 8(a)] and port-2 excitation [Fig. 8(b)], the switches ON are replaced by a 2-mm long metal strip, and the switches OFF are replaced by a 2-mm long gap. The antenna's inverted-L strip is printed on a 0.8-mm thick FR4 substrate, and the chip elements ($L_1 = 18$ nH, $L_2 = 1.5$ nH, $C_1 = 8.2$ pF,

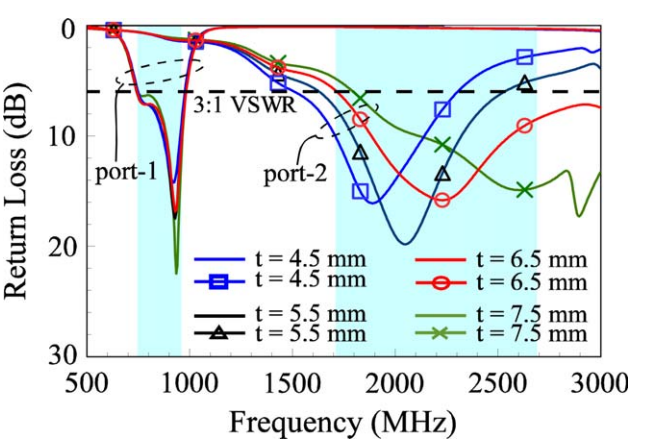


**Figure 7** Simulated return loss as a function of the supporting metal plate size for the antenna. [Color figure can be viewed in the online issue, which is available at wileyonlinelibrary.com]

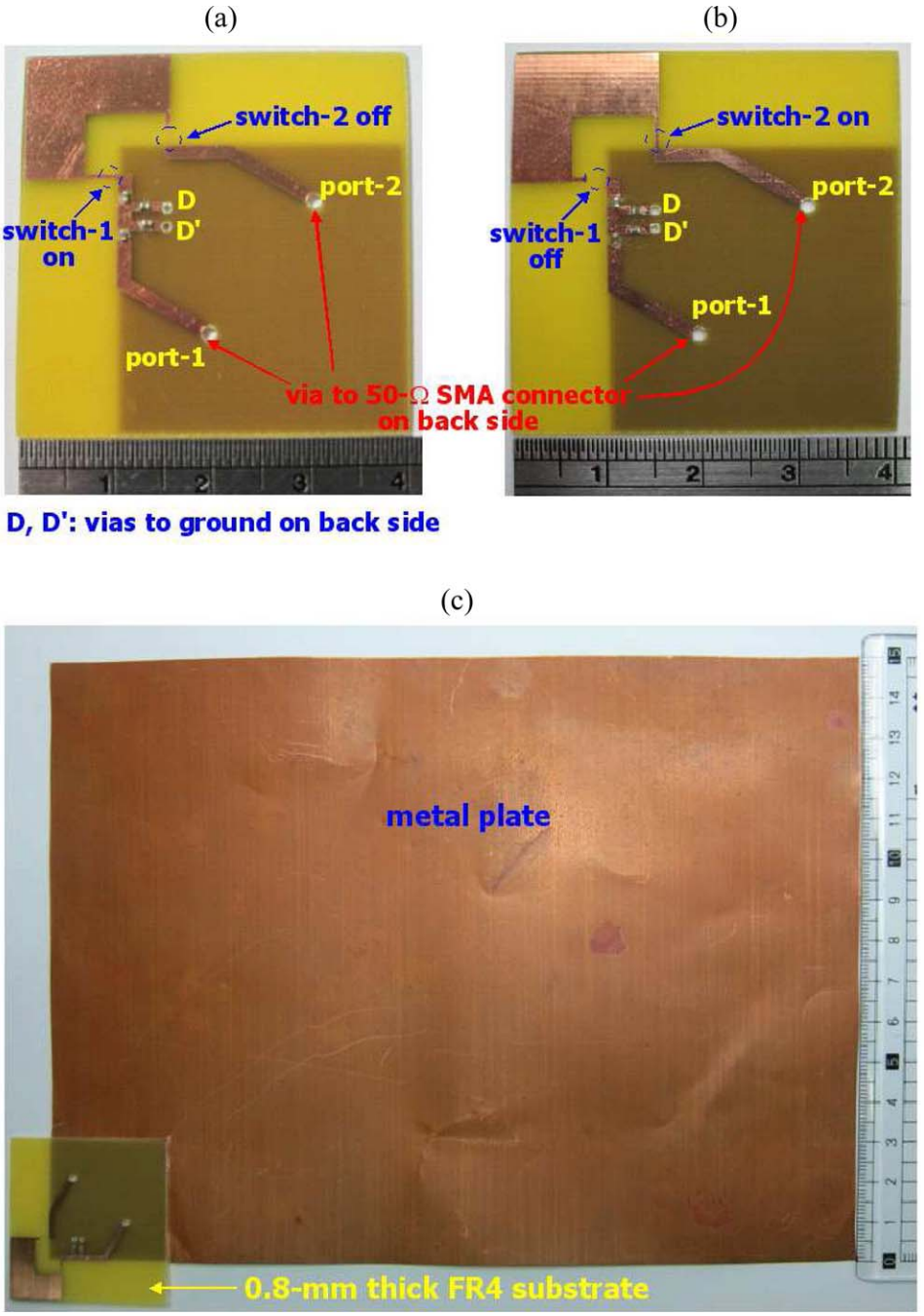


**Figure 8** Photos of the fabricated antenna. (a) Port-1 excitation. (b) Port-2 excitation. (c) Antenna with the metal plate in the experiment. [Color figure can be viewed in the online issue, which is available at wileyonlinelibrary.com]

$C_2$ = 10 pF) of the matching circuit are mounted thereon. Figure 8(c) shows the antenna with the metal plate in the experiment, and the measured return loss for the fabricated antenna is shown in Figure 9. Wide lower and higher bands are obtained for the antenna. Based on 3:1 VSWR, the impedance bandwidth covers the 746–960 MHz for the LTE band13/GSM850/900 operations and the 1710–2690 MHz for the GSM1800/1900/UMTS/LTE2300/2500 operations. The measured results also agree with the simulated results shown in Figure 2.

The measured antenna efficiency for the fabricated antenna is shown in Figure 10. The antenna efficiency is the total efficiency including the mismatching losses. The antenna efficiency is about 50–79% and 65–85% for frequencies over the lower and higher bands, respectively. The measured antenna efficiency is with small discrepancies to the simulated results shown in Figure 4. Figure 11 shows the measured radiation patterns for the antenna. Results for three principal planes at representative frequencies at 925 and 1920 MHz are shown. Both $E_\theta$ and $E_\phi$ for three principal planes are normalized with respect to the same maximum value. It is noted that in the *x-y* plane, comparable $E_\theta$ and $E_\phi$ radiation are seen. This is largely related to the strip monopole disposed at around a corner of the supporting metal plate of the display, such that the surface currents in both the horizontal and vertical directions can be excited thereon and hence strong radiation in both the horizontal and vertical directions can be obtained. This behavior will be attractive for practical applications since the wave propagation environment is usually complex for mobile communications.

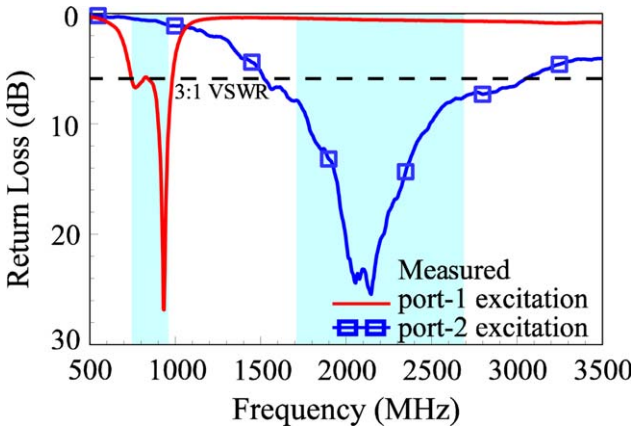


**Figure 9** Measured return loss for the fabricated antenna. [Color figure can be viewed in the online issue, which is available at wileyonlinelibrary.com]

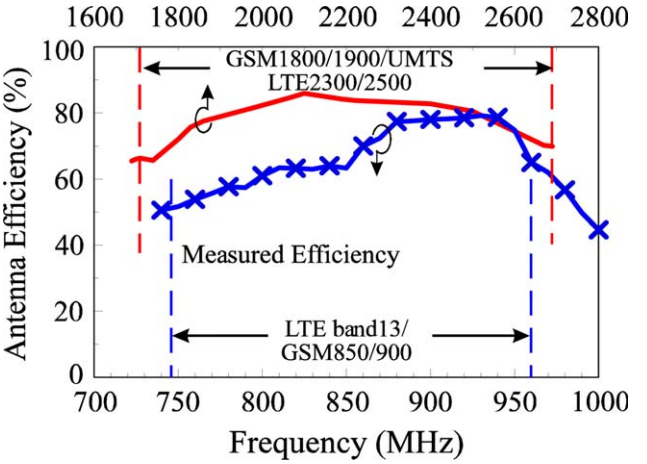


**Figure 10** Measured antenna efficiency for the fabricated antenna. [Color figure can be viewed in the online issue, which is available at wileyonlinelibrary.com]

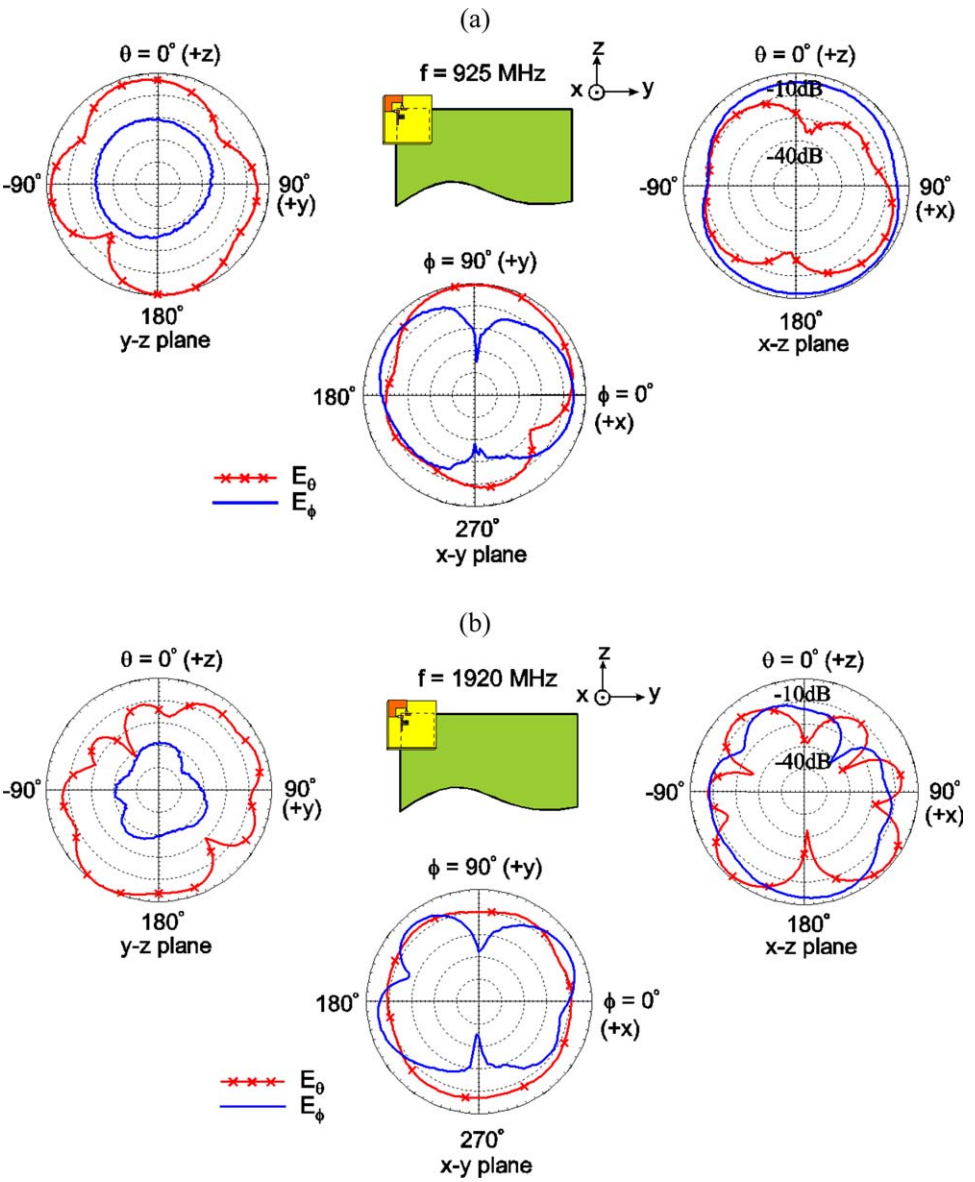


**Figure 11** Measured radiation patterns for the fabricated antenna. (a) 925 MHz. (b) 1920 MHz. [Color figure can be viewed in the online issue, which is available at wileyonlinelibrary.com]

## 4. CONCLUSION

A dual-feed small-size strip monopole antenna suitable for LTE/WWAN operation in the tablet computer has been proposed and studied. The strip monopole is easy to implement owing to its small size, simple shape, and planar structure, yet it can provide two wide operating bands (746–960/1710–2690 MHz) for LTE/WWAN operation. It has been shown that the strip monopole configured to be an inverted-L shape and mounted at one corner of the display's supporting metal plate can be fed at its two ends, which can be connected to ON/OFF switches such as the switching diodes for controlling the lower- and higher-band operations. The lower band is aided by a wideband matching circuit to achieve wideband operation, while the higher band requires no matching circuits for wideband operation. Fabricated prototype of the proposed antenna has been tested, and acceptable impedance matching and antenna efficiency for frequencies over the desired operating bands have been observed. Good radiation characteristics for frequencies over the operating bands have also been obtained. With the obtained results, the proposed antenna will be promising for tablet computer applications, especially for the slim tablet computer applications.

## REFERENCES


1. K.L. Wong, Planar antennas for wireless communications, Wiley, New York, 2003.
2. A. Andújar and J. Anguera, Multiband coplanar ground plane booster antenna technology, Electron Lett 48 (2012), 1326–1328.
3. A. Andújar, J. Anguera, and C. Puente, Ground plane boosters as a compact antenna technology for wireless handheld devices, IEEE Trans Antennas Propag 59 (2011), 1668–1677.
4. D.H. Schaubert, F.G. Farrar, A. Sindoris, and S.T. Hayes, Microstrip antennas with frequency agility and polarization diversity, IEEE Trans Antennas Propag 29 (1981), 118–123.
5. E. Palantei, D.V. Thiel, and S.G. O'Keefe, Rectangular patch with parasitic folded dipoles: A reconfigurable antenna, Proceedings 2008 iWAT, International Workshop on Antenna Technology, Chiba, Japan, 2008, pp. 251–254.
6. Y.K. Park and Y. Sung, A reconfigurable antenna for quad-band mobile handset applications, IEEE Trans Antennas Propag 60 (2012), 3003–3006.
7. ANSYS HFSS. Ansoft Corp., Pittsburgh, PA. Available at: http://www.ansys.com/products/hf/hfss/.
8. K.L. Wong, Y.W. Chang, and S.C. Chen, Bandwidth enhancement of small-size WWAN tablet computer antenna using a parallel-resonant spiral slit, IEEE Trans Antennas Propag 60 (2012), 1705–1711.
9. K.L. Wong, T.J. Wu, and P.W. Lin, Small-size uniplanar WWAN tablet computer antenna using a parallel-resonant strip for bandwidth enhancement, IEEE Trans Antennas Propag 61 (2013), 492–496.




# STRAIN MEASUREMENT BASED ON SMS FIBER STRUCTURE SENSOR AND OTDR

**A. M. Hatta,[1,2] H. E. Permana,[1] H. Setijono,[1] A. Kusumawardhani,[1] and Sekartedjo[1]**
[1] Department of Engineering Physics, Faculty of Industrial Technology, Institut Teknologi Sepuluh Nopember, Surabaya, Indonesia; Corresponding author: amhatta@ep.its.ac.id
[2] Department of Physics, Faculty of Science, Jazan University, Jazan, Saudi Arabia

*Received 11 March 2013*

**ABSTRACT:** *This article presents a strain measurement method using a singlemode-multimode-singlemode fiber structure sensor and an optical time domain reflectometer. A strain measurement range of 0–1000 με can be achieved with a resolution of better than 10 με. Using this method, a quasi-distributed strain measurement can be carried out which is useful for a bridge or a civil structure strain monitoring.* © 2013 Wiley Periodicals, Inc. Microwave Opt Technol Lett 55:2576–2578, 2013; View this article online at wileyonlinelibrary.com. DOI 10.1002/mop.27903

**Key words:** *fiber optics; multimode interference; strain sensor*

## 1. INTRODUCTION

A strain measurement in a level of με (microstrain) unit is needed in many areas such as in a bridge or civil structure monitoring, material processing, and others applications [1]. While compared to the conventional strain sensors, fiber optics strain sensors have some advantages of immune from electromagnetic interference, small size and lightweight, can be used for remote measurement, and multiple sensors can be placed and interrogated in a single fiber network [2]. A fiber-Bragg grating (FBG) strain sensor has been utilized widely and has been implemented to monitor strain condition in many bridges and buildings [1]. In implementation of the FBG strain sensor, it is needed an interrogator system that can detect the reflected wavelength shifts due to the applied strain changes. This interrogator system is quite complicated and also the FBG itself requires fabrication complex process [2].

Recently, a singlemode-multimode-singlemode (SMS) fiber structure has been proposed as a strain sensor [3,4]. Other application based on the strain effect for a voltage measurement is also reported [5]. The SMS fiber structure can be fabricated with a simple process compared to the FBG. A strain or temperature coefficient of the SMS fiber structure has similar value when compared to the FBG [3].

In the strain measurement using the SMS fiber structure sensor, it has been proposed the interrogator system based on a wavelength shift measurement using an optical spectrum analyzer [3] and an intensity measurement using an optical power meter [4]. Approaches in [3,4] can only be used for single point measurement. It is necessary to further investigate a quasi-distributed strain measurement based on the SMS fiber structure. One possible solution is utilizing an optical time domain reflectometer (OTDR). It is reported that the OTDR has been utilized as an interrogator for the quasi-distributed sensing system [6,7]. Normally, the OTDR is used to determine events in the optical fiber network such as connection, splicing, cracks, and so forth. These events can be detected by measuring the reflected light/return loss from the light source in the OTDR unit. The SMS fiber structure's connection and the applied strain on the SMS fiber structure can be detected as an event in the OTDR. In this article, the strain measurement method using the SMS fiber structure sensor and an OTDR as the interrogator is presented.

## 2. EXPERIMENTAL SET-UP

A schematic structure of an SMS fiber structure is shown in Figure 1(a). It is formed by splicing a section of graded-index multimode fiber (MMF) between two pieces of standard singlemode-fiber (SMF). The SMF type of SMF28 (ITU-T recommendation G.655) and the MMF graded index (ITU-T recommendation G.651) were used. The SMS fiber structure described earlier is fabricated using a precision Fitel Nc S324 fiber cleaver and a compact fusion splicer of Sumitomo Electric type-25e.

An MMF length of 40, 60, 80, and 100 mm were chosen because of the easiness of its splicing process. The two SMF lengths of circa 250 m were used to construct the SMS fiber structure. The experimental setup was built and is shown in Figure 1(b). The SMS fiber structure was attached to a fixed stage